Covalency effects in transition-metal perovskitelike compounds: Partial densities of p and d states and photoelectron valence-band spectra

P. Pertosa and G. Hollinger

Institut de Physique Nucléaire and Institut de Physique Nucléaire et de Physique des Particules (Centre National de la Recherche Scientifique), Université Lyon I, 43 Boulevard du 11 Novembre 1918, 69621 Villeurbanne, France

F. M. Michel-Calendini

Laboratoire d'Electronique et Physique des Solides, Université Lyon I, 43 Boulevard du 11 Novembre 1918, 69621 Villeurbanne, France

(Received 8 June 1978)

The evolution of x-ray-photoelectron (XPS) valence-band spectra for the series of perovskitelike compounds $BaTiO_3$, $KNbO_3$, $KTaO_3$, WO_3, and ReO_3 gives evidence for quite important covalency effects due to the spatial overlap of metal md and oxygen $2p$ states. Theoretical partial densities of states of d and p character allow an explanation of the experimental results when transition-matrix-element effects are taken into account. These are introduced by using atomic cross sections for the corresponding partial transition probabilities in a simple model which is justified in the XPS regime. We discuss the cross-section values and the atomic-population analysis. The uv-photoelectron valence-band spectrum of WO_3 compared to the XPS one confirms the validity of the calculated partial densities of states. The case of ReO_3 already given in the literature is included in this work; the theoretical density of states is computed again with slight modifications in order to improve the agreement with published experimental results and to test the influence of two different population analyses.

I. INTRODUCTION

It is at present well known that valence-band spectra obtained by x-ray-photoelectron spectroscopy (XPS) or uv-photoemission spectroscopy (UPS) may be distorted, sometimes severely, by photoionization transition probabilities compared to one-electron densities of states. This problem has been largely discussed in the case of small-molecule valence shells[1-3] and to a lesser extent in several cases of crystalline compounds whose valence-band shapes and intensities were found to vary with the incident-photon energy.[4,5] In the same way, recent studies using angle-resolved photoemission have obtained more precise band-structure information for fixed directions in the Brillouin zone.[6]

This paper aims to show the improvement of theoretical densities of states (DOS) when photoionization cross sections are taken into account. We illustrate this phenomenon on a series of ABO_3 perovskite-type compounds, the valence bands of which are well described by the md-$2p$ mixing of oxygen $2p$ orbitals and B-atom md orbitals, where B is a transition metal. We discuss here the results for three ternary oxides, namely, $BaTiO_3$, $KNbO_3$, and $KTaO_3$, whose XPS valence bands have been previously given.[7,8]

We also present the case of the distorted perovskitelike trioxide WO_3, for which we obtained both XPS and UPS valence bands: comparison of these two spectra gives evidence for cross-section variations with incident-photon energy and permits one to test the validity of theoretical DOS. The discussion is then extented to the cubic perovskite-like rhenium trioxide ReO_3, which has already been treated,[9] but on which we show the influence of two different electronic-population analyses in the DOS. The obvious difference between the ReO_3 valence band and the others is the presence of the Re $5d$ conduction band containing one electron per unit cell which confers to this compound its metallic character.

The evolution of valence-band spectra along the transition-metal series Ti, Nb, Ta, W, Re, and comparison with computed DOS give evidence for quite important covalency effects in these compounds.

II. EXPERIMENTS

XPS valence-band spectra were obtained with a HP 5950A spectrometer. The incident x-ray is the monochromatized Al $K\alpha$ radiation. The total spectrometer resolution is estimated to be 0.60 eV. The $BaTiO_3$, $KNbO_3$, and $KTaO_3$ samples were transparent colorless single crystals. The sample surface cleaning procedure described in detail elsewhere[7] is performed by scraping the crystal with a diamond tool. This preparation is believed to be sufficiently indicative of the bulk properties to allow meaningful comparison of XPS experiments with theory.

In the case of WO_3 two samples were prepared. For XPS experiments the oxide was grown in air at a temperature of 500 °C; the still-hot sample

was immediately introduced in the 3×10^{-9}-Torr vacuum of the spectrometer chamber. No carbon pollution is visible on the valence-band spectrum. For UPS experiments the oxide was thermally grown at the same temperature in the preparation chamber of a V. G. ESCA III spectrometer under a pressure of 1 atm of pure oxygen. The spectrum was recorded with the He II (40.8 eV) radiation. For ReO_3, as already reported in Sec. I, we used the XPS spectrum obtained by Wertheim *et al.*[9] on a vacuum-cleaved crystal.

A background subtraction is applied on smoothed experimental valence bands as described previously.[7]

III. DENSITIES OF STATES AND TRANSITION PROBABILITIES

Electronic levels $E_n(\vec{k})$ and relevant densities of states for $BaTiO_3$ and $KNbO_3$ are computed using a semiempirical linear-combination-of-atomic-orbitals–molecular-orbital tight-binding method. Details of the calculation are given in Ref. 7, where the effects of the various interatomic interaction matrix elements are analyzed. Besides the B-ion md orbitals and oxygen $2p$ orbitals, the ms and mp orbitals of the B ion, $2s$ orbitals of oxygen as well as ns and np orbitals of the A ion were taken into account. The admixture of these orbitals in the mainly B-md–O-$2p$ valence band is small and chiefly acts on the energy-level positions. So, in the present DOS we neglect the A-ion orbitals and the ms and mp orbitals of the B ion. The only difference with the preceding work is a slight readjustment of the $pd\sigma$ and $pd\pi$ parameters, for $BaTiO_3$, in order to better reproduce the high-binding-energy tail of the experimental valence band without modifying noticeably the electronic band scheme.

In the case of $KTaO_3$ and ReO_3 we merely used the two-center adjusted parameters determined by Mattheiss[10] to fit the optical data[11], and we computed the energy levels by the classical tight-binding interpolation scheme. As pointed out by Wertheim *et al.*,[9] the calculated O-$2p$–Re-$5d$ band gap of ReO_3 is too small. Therefore, we attempted a better energy adjustment. As a consequence, the intensity ratio of the Re $5d$ band to the O $2p$ band is slightly increased, drawing the DOS closer to experiment. We shall come back to this point later.

Photoionization cross sections are introduced in DOS computations in the way first proposed in Ref. 1 and successfully applied to molecular valence shells. The monoelectronic orbital $\Phi_{n\vec{k}}$ and the photoionization cross section $\sigma_{n\vec{k}}$ relative to eigenvalue $E_{n\vec{k}}$ are given by

$$\Phi_{n\vec{k}}=\sum_{i,\mu} D^{\mu}_{ni}(\vec{k})\chi^{\mu}_{i}(\vec{k}) , \tag{1}$$

$$\sigma_{n\vec{k}}=\sum_{i,\mu} P^{\mu}_{ni}(\vec{k})\sigma^{\mu}_{i} . \tag{2}$$

D and P matrices stand, respectively, for the expansion coefficients and for the electronic population of the $\chi^{\mu}_{i}(\vec{k})$ Bloch atomic orbital in the $\Phi_{n\vec{k}}$ molecular orbital. σ^{μ}_{i} is the atomic photoionization cross section for subshell i of atom μ. The DOS modulated by cross sections (hereafter denoted DOSC) is then of the form

$$N_c(E)=\sum_{n}\sum_{\vec{k}}\sigma_{n\vec{k}}\delta(E-E_{n\vec{k}}) , \tag{3}$$

where the second summation spans on $\vec{k}$ vectors in the first Brillouin zone. An alternative form of Eq. (3) is

$$N_c(E)=\sum_{i,\mu}\sigma^{\mu}_{i}N^{\mu}_{i}(E) , \tag{4}$$

where $N^{\mu}_{i}(E)$ stands for the partial DOS of χ^{μ}_{i} character. The summation $2\sum N^{\mu}_{i}(E)\Delta E$ in the energy range of a given occupied band leads to the electronic population P^{μ}_{i} of the χ^{μ}_{i} orbital in this band.

Improvements of this semiempirical approach have been worked out by several authors with varying degrees of approximation for computing with more theoretical justification valence-orbital photoionization cross sections in arbitrary molecules.[12-14] For crystals the treatment is more complex due to the $\vec{k}$ and angle dependence of transition-matrix elements. This problem has been discussed, particularly by workers having performed angle-resolved photoemission energy distributions on one-element single crystals.[6,15] If we transpose in the case of crystals the model of Schweig and Thiel[14] established for the treatment of molecules, it can be shown that the simple formulation of Eq. (2) is a good approximation for comparison of theoretical DOS with XPS experiments.

In the time-dependent first-order perturbation scheme involving the dipole, plane-wave final state, Koopmans, and initial Bloch orbital approximations, the differential cross section can be written

$$\frac{d\sigma_{n\vec{k}}}{d\Omega}\propto(\vec{u}\cdot\vec{q})^2\delta(\vec{q}-\vec{k}-\vec{G}) \times\sum_{i,\mu}\sum_{j,\nu}D^{*\mu}_{ni}(\vec{k})D^{\nu}_{nj}(\vec{k})M^{*\mu}_{i}M^{\nu}_{j} \times Y^{*}_{i}(\hat{q})Y_{j}(\hat{q})e^{-i\vec{q}\cdot\vec{R}_{\nu\mu}} , \tag{5}$$

where $\vec{u}$ is the polarization of the incident light, $\vec{q}$ the momentum of the photoejected electron, $\vec{G}$

are reciprocal-lattice vectors, and $R_{\nu\mu}$ the interatomic vector $(\vec{R}_\mu - \vec{R}_\nu)$. The $Y_i(\hat{q})$ are normalized spherical harmonics and M_i^μ are total atomic transition-matrix elements for subshell i of atom μ.

In the present experiments which are not angle resolved, we use angle-averaged matrix elements although we worked on $BaTiO_3$, $KNbO_3$, and $KTaO_3$ single crystals. This is entirely justified for several reasons: (i) sample cleaning by scraping the surface with a diamond tool partially destroys the perfect crystal face; (ii) the crystal orientation is not a particular one; and (iii) as suggested by Shevchik[16] the phonon-assisted indirect transition process at XPS energies increases the sampling of the first Brillouin zone. These considerations combined with the 8° angular acceptance of the spectrometer ensure that the whole Brillouin zone is explored for a given energy. We confirmed this fact by comparing $BaTiO_3$ spectra obtained from a ceramic (polycrystalline) sample and from a single crystal: the only difference lies in the surface cleanliness which is better achieved for the monocrystal sample.

When integrating Eq. (5) over all angles the δ function coming from the Bloch form of atomic orbitals and representing the $\vec{k}$ conservation, may disappear at XPS energies where $q \gg k$. This permits averaging and leads to

$$\sigma_{n\vec{k}} \propto \sum_{i,\mu} \sum_{j,\nu} D_{ni}^{*\mu}(\vec{k}) D_{nj}^{\nu}(\vec{k}) M_i^{*\mu} M_j^{\nu} I_{ij}\,, \tag{6}$$

where I_{ij} involves diffraction effects depending on the photoemitted electron wave vector and on the interatomic distance $R_{\nu\mu}$.[14] For low values of $qR_{\nu\mu}$, the I_{ij} functions oscillate greatly; for large values (XPS: $q = 19.7$ Å^{-1}) they vanish and there remain in Eq. (6) only one-center terms in the form

$$\sigma_{n\vec{k}} \propto \sum_{i,\mu} D_{ni}^{*\mu}(\vec{k}) D_{ni}^{\mu}(\vec{k}) M_i^{*\mu} M_i^{\mu}\,, \tag{7}$$

where the product $M_i^{*\mu} M_i^{\mu}$ is proportional to σ_i^μ. This last formulation is similar to Eq. (2), in which P_{ni}^μ is the population of atomic orbital i. From Eq. (7) it appears that the population analysis should be a "net" one in terms of a Mulliken analysis, while the semiempirical character of Eq. (2) cannot indicate whether a "net" or a "gross" population has to be used. Recall that the net population in simply the one-center term $D_{ni}^{*\mu} D_{ni}^{\mu}$. The overlap population $\sum_{j,\nu\neq\mu} D_{ni}^{*\mu} D_{nj}^{\nu} S_{ij}^{\mu\nu}$, where $S_{ij}^{\mu\nu}$ are overlap integrals, gives the gross population when added to the net one. We computed here, both "gross" and "net" populations; as will be discussed in Sec. IV the differences are not significant, except for ReO_3.

TABLE I. Atomic cross sections per electron relative to oxygen 2p from Scofield (Ref. 17) and deduced from experiments.

μ, i	O 2p	Ti 3d	Nb 4d	Ta 5d	W 5d	Re 5d
σ_i^μ Scofield	1.0	1.4	10.3	19.2	22.5	25.9
σ_i^μ Experiments	1.0	4–6	10–12	23–26		

The last problem is the choice of the atomic cross sections which will be used in the calculations. In the original work of Gelius,[1] relative experimental atomic cross sections measured from XPS intensities were used to deduce the molecular ones. For transition-metal md orbitals such experimental values are not available and in a first approach we used the Hartree-Slater values computed by Scofield.[17] We think that even if these calculated cross sections are not always good in an absolute sense, their relative values will properly, reproduce trends along a series of compounds. Cross sections per electron, relative to oxygen 2p taken as unity, are reported in Table I.

IV. RESULTS AND DISCUSSION

XPS valence bands for $BaTiO_3$, $KNbO_3$, and $KTaO_3$ are compared to theoretical results in Figs. 1–3, respectively. In each figure, curve a represents total and partial DOS of metal md and oxygen 2p character obtained from a gross population analysis. Total and partial DOSC, including Scofield's cross sections, are pictured on curve b. Curve c shows the XPS valence-band spectrum.

It appears that the total DOS and DOSC are not too different for $BaTiO_3$ allowing a straightforward comparison between the computed density of states and XPS measurements. This is no longer true for $KTaO_3$ which is more sensitive to 5d-state admixture in the 2p band due to the large transition probability compared to the O-2p one. $KNbO_3$ is an intermediate case, but here also, transition probability effects are important enough to distort sensibly the DOS curve.

Nevertheless, for $BaTiO_3$, the value $\sigma_{3d}^{\mathrm{Ti}} = 1.4$ seems a little too low and in Fig. 4 we compare the results obtained for this value and for $\sigma_{3d}^{\mathrm{Ti}} = 4.0$ which gives the best fit with the XPS spectrum. In Fig. 4 theoretical DOSC are enlarged with a Gaussian function of 1.2-eV FWHM instead of 0.6 eV in order to give a better visualization of the accord with experiments. The theoretical curves are narrower than the experimental ones

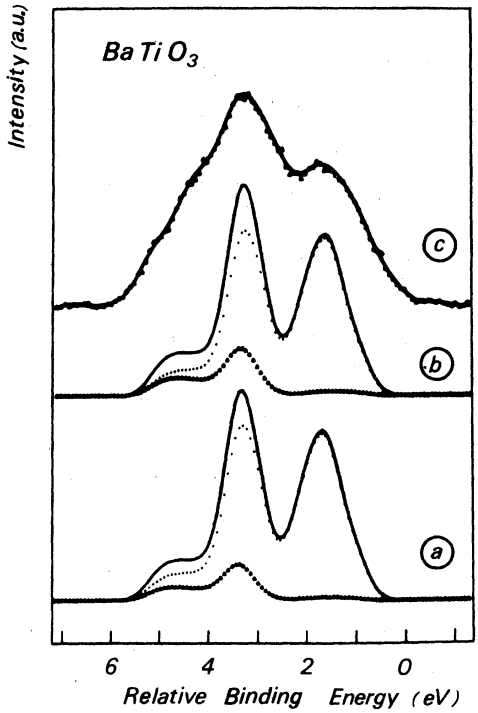

FIG. 1. XPS valence band and theoretical DOS for $BaTiO_3$. Curve a: total DOS (—), partial $2p$ DOS (·····), partial md DOS (▲▲▲). Curve b: total DOSC (—), partial $2p$ DOSC (····), partial md DOSC (▲▲▲). Curve c: experimental spectrum.

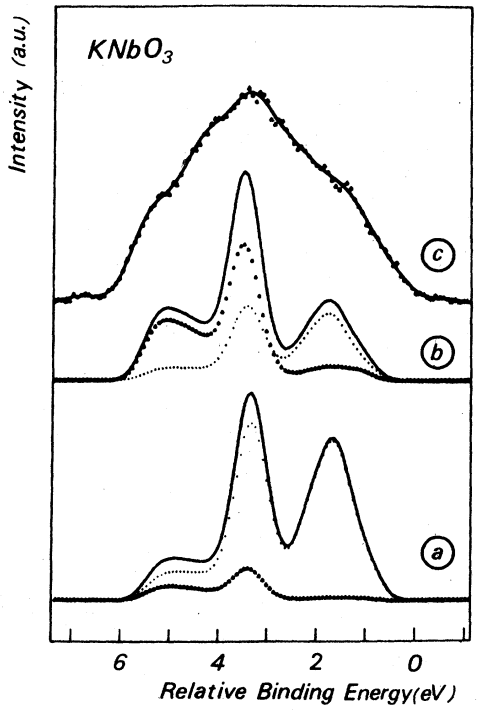

FIG. 2. XPS valence band and theoretical DOS for $KNbO_3$. For details of curves a, b, c, see Fig. 1.

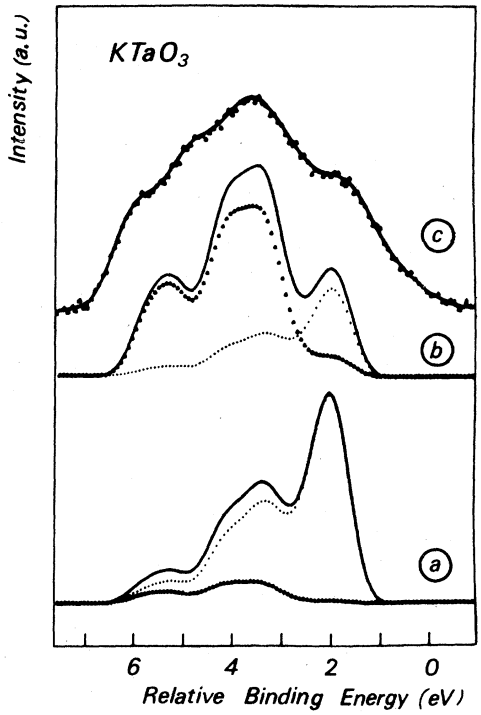

FIG. 3. XPS valence band and theoretical DOS for $KTaO_3$. For details of curves a, b, c, see Fig. 1.

even when the spectrometer resolution is taken into account. We think that this discrepancy is due both to the calculation and to physical phenomena (natural widths of states, broadening due to phonon disorder in XPS regime).

When partial DOS are obtained through a net population analysis instead of a gross one, this does not induce important modifications in the valence-band shapes. One obtains chiefly a slight decrease of the md contribution in the high-binding-energy tail of the valence band, that it to say in the region of $pd\sigma$ interactions. The fit of theoretical results with experiments can be achieved again by choosing a set of σ_{md} atomic cross sections whose values are slightly higher than those used for a gross population analysis. For ReO_3 the problem is a little different due to the presence of the Re $5d$ conduction band besides the mainly oxygen $2p$ valence band which imposes an additional constraint. We now discuss the case of this metallic compound.

Wertheim *et al.* obtained relative agreement with experiments by taking the cross section σ_{5d}^{Re} of the order of 40, a value considerably greater than Scofield's (Table I). But even if we neglect totally the O-$2p$ contribution ($\sigma_{5d}^{Re} \to \infty$) the theoretical intensity ratio of the $5d$ conduction band (CB) to the $2p$ valence band (VB) remains too low compared with experiments. That is the reason why

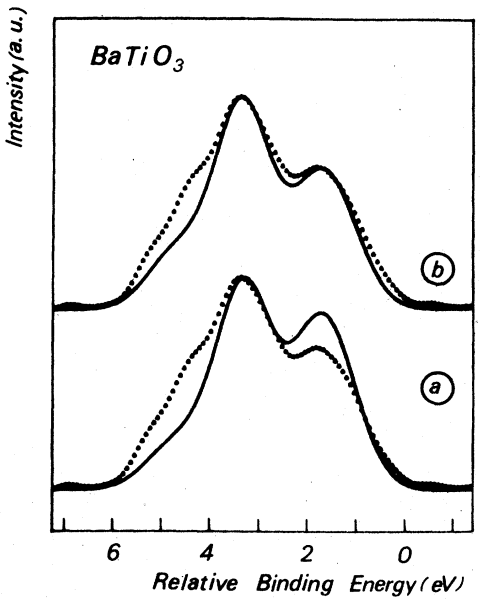

FIG. 4. XPS valence band of $BaTiO_3$ (▲▲▲) and theoretical DOSC (—), for $\sigma_{3d}^{Ti}=1.4$ (curve *a*) and $\sigma_{3d}^{Ti}=4.0$ (curve *b*).

we attempted a better energy adjustment of the Mattheiss' parameters by varying slightly the diagonal integrals $(5d,5d)$ and $(2p,2p)$ and transfer integrals $pd\sigma$ and $pd\pi$ of $5d$ and $2p$ orbitals. We increased, in particular, the $5d$-$2p$ band-gap energy by 0.65 eV according to XPS results.[9] We must note that this band gap could not be obtained on the basis of optical data.[11] As a consequence of these parameter modifications the $5d$-$2p$ mixing diminishes and the CB to VB ratio is then enhanced as it can be seen on Fig. 5 (curve *b*) compared to the DOSC obtained from the original Mattheiss' computation (curve *a*). The last improvement is obtained by computing net populations rather than gross populations. The result is shown on curve *c* where the CB to VB ratio is increased leading to quite good agreement with experiments.

The present DOSC seem to correctly reproduce the experimental results for this series of perovskitelike compounds. Moreover, the shape of the O-$2p$ partial DOS is confirmed by the UPS spectrum we obtain for WO_3: it is well known that the cross-section ratio $\sigma_{2p}^{O}/\sigma_{md}^{B}$ is much more important in the UPS than in the XPS energy range and the UPS valence-band spectrum is then mostly representative of the oxygen-$2p$ DOS. Although a calculated DOS is not available for WO_3, we can compare in a first approximation, the UPS valence-band spectrum of WO_3 to the partial DOS of oxygen-$2p$ character of $KTaO_3$ whose electronic structure is expected to be very similar. In Fig. 6, XPS

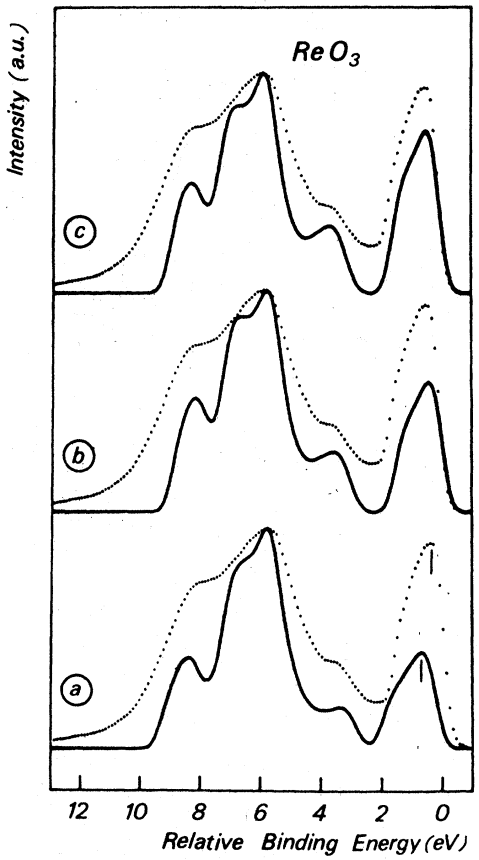

FIG. 5. XPS valence band of ReO_3 from Ref. 9 (····) and theoretical DOSC (—): from Ref. 9 (curve *a*); gross population analysis (curve *b*); net population analysis (curve *c*).

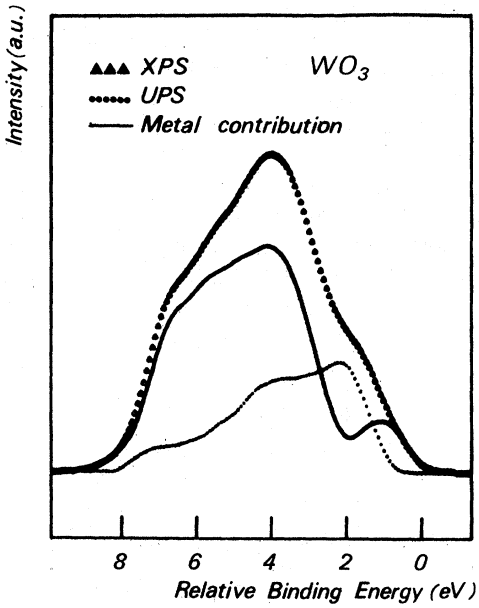

FIG. 6. XPS and UPS valence bands of WO_3.

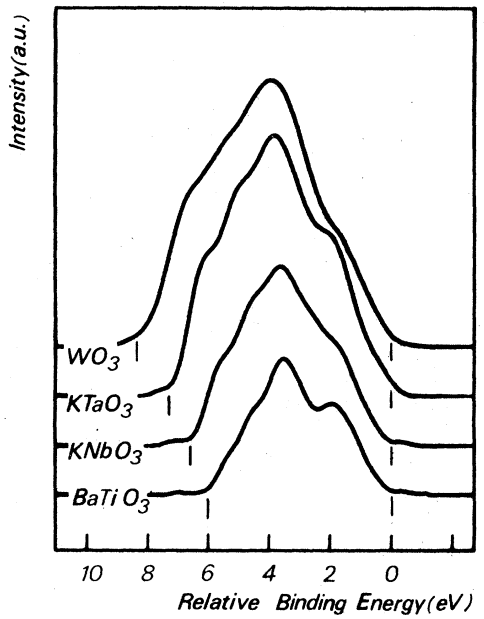

FIG. 7. Normalized XPS valence bands for the series $BaTiO_3$, $KNbO_3$, $KTaO_3$, WO_3.

and UPS valence-band data for WO_3 have been superimposed. The normalization of the two spectra is made on the structure of lower binding energy which is, in each case, of nearly pure oxygen $2p$ character. By subtracting the two spectra we obtain approximately the shape of the tungsten $5d$ contribution. We must note that this partial metal density may be somewhat distorted by the fact that the UPS spectrum is a little narrower than the XPS one, and is underestimated by the fact that there certainly remain some metal contributions in the UPS spectrum. However, the d contribution reproduces in an adequate way the main features of the $5d$ partial DOS of $KTaO_3$ [Fig. 3(b)].

The approximations of the model used in this work to introduce photoionization probabilities were shown to be suitable for the XPS field. One should ask if it is still valid for the UPS energy range. From several experimental results[4,5,18] it seems that, as long as the incident-photon energy is not smaller than about 20 eV, the model is credible. In Ref. 18, in particular, it is shown that the interference terms are small over the whole Brillouin zone and contribute less than 20% to the transition probabilities for photon energies ranging from 16.8 to 48.4 eV. For XPS, this contribution is certainly less than 5% considering the plots of I_{ij} functions versus $qR_{\nu\mu}$.[14]

Finally, in order to give evidence for p-d overlap covalency effects in these compounds independent of calculated DOS, we have normalized all the valence-band spectra with respect to the oxygen $2s$ peak which can be considered to be of pure $2s$ character. It is difficult to achieve an exact normalization because of the problem of background subtraction under the oxygen $2s$ peak whose tail overlaps with neighboring signals especially for $KTaO_3$, where it lies in the lower binding energy tail of the huge Ta-$4f_{7/2}$ peak.

The comparison is presented on Fig. 7 where the normalized valence bands are shown. It clearly appears that valence-band intensities increase from titanium to tungsten perovskites, due to transition probability effects. We give in Table II the VB to O-$2s$ intensity ratios. Simultaneous enlargement of bandwidths also reported in Table II shows that $pd\sigma$ and $pd\pi$ interactions are stronger when going from light to heavy transition metal elements.

Thus, the contribution of metal d states in the valence bands of these compounds seems to be important, supporting the calculated atomic populations presented in Table III. These populations, combined with the experimental VB to O-$2s$ ratios (Table II) allow the determination of a set of semiempirical relative cross sections for XPS experiments with Al $K\alpha$ radiation. When the ratio $\sigma^{O}_{2s}/\sigma^{O}_{2p}$ is taken to be of the order of 9.0,[1,19] the set of experimental cross sections reported in Table I is obtained. These values are not too far from Scofield's data except for titanium: here, the calculated value is close to the value of 4.0 giving the best fit between theory and experiment, as outlined in Fig. 4. For tungsten (and possibly for rhenium) Scofield's values are lower than experimental ones. We must note that this determination of transition probabilities depends

TABLE II. Experimental VB to O-$2s$ intensity ratios and valence-band widths (eV).

Compound	$BaTiO_3$	$KNbO_3$	$KTaO_3$	WO_3
VB to O $2s$	0.48 ± 0.05	0.69 ± 0.05	1.18 ± 0.1	1.32 ± 0.03
Valence-band widths (eV)	6.0 ± 0.1	6.5 ± 0.1	7.2 ± 0.2	8.3 ± 0.2

TABLE III. Gross-atomic-population analysis for each compound, and net populations of ReO_3. VB and CB denote the valence band (mainly O $2p$) and the conduction band.

Atomic orbital	$BaTiO_3$	$KNbO_3$	$KTaO_3$	ReO_3 (gross)	ReO_3 (net)
O $2s$ (VB)	0.02	0.03	0.09	0.09	
O $2p$ (VB)	15.89	15.92	15.93	14.94	14.50 [a]
B md (VB)	2.09	2.05	1.98	2.97	2.44
O $2p$ (CB)				0.20	0.19
B md (CB)				0.80	0.80
Total	18.00	18.00	18.00	19.00	17.93

[a] This value is the sum $P^{o}_{2s} + P^{o}_{2p}$.

on the set of atomic populations and we cannot obtain experimentally both populations and cross sections. Quantities such as populations are not without ambiguities and have no unique meaning. They depend on the basis set and in particular if it is orthogonalized or not. Nevertheless, two different population analyses lead to approximately the same results, even if a net analysis seems better for ReO_3. Moreover, in the XPS field we are in a favorable case where the simple model of Eq. (7) gives satisfying results because cross sections are not too sensitive to atomic-orbital variations in the bonding region, as discussed by several authors,[2,20] and do not vary appreciably between the bottom and the top of valence bands. Coming back to the atomic populations of Table III, we cannot compare precisely the values for $BaTiO_3$ and $KNbO_3$ obtained from our tight-binding computations with the ones of $KTaO_3$ and ReO_3 obtained from the augmented-plane-wave calculations of Mattheiss.[10] Nevertheless, the whole of these results is coherent and the DOS demonstrate a p-d overlap covalency consistent with the XPS valence-band spectra.

[1] U. Gelius, in *Electron Spectroscopy*, edited by D. A. Shirley (North-Holland, Amsterdam, 1972), p. 311.
[2] W. C. Price, A. W. Potts, and D. G. Streets, in *Electron Spectroscopy*, edited by D. A. Shirley (North-Holland, Amsterdam, 1972), p. 187.
[3] M. S. Banna, B. E. Mills, D. W. Davis, and D. A. Shirley, J. Chem. Phys. 61, 4780 (1974).
[4] D. E. Eastman and J. L. Freeouf, Phys. Rev. Lett. 34, 395 (1975).
[5] A. Goldmann, J. Tejeda, N. J. Shevchik, and M. Cardona, Phys. Rev. B 10, 4388 (1974).
[6] G. Apai, J. Stöhr, R. S. Williams, P. S. Wehner, S. P. Kowalczyk, and D. A. Shirley, Phys. Rev. B 15, 584 (1977).
[7] P. Pertosa and F. M. Michel-Calendini, Phys. Rev. B 17, 2011 (1978).
[8] F. M. Michel-Calendini, P. Pertosa, and G. Metrat, Ferroelectrics (to be published).
[9] G. K. Wertheim, L. F. Mattheiss, M. Campagna, and T. P. Pearsall, Phys. Rev. Lett. 32, 997 (1974).
[10] L. F. Mattheiss, Phys. Rev. B 6, 4718 (1972).
[11] S. K. Kurtz, T. C. Rich, and W. J. Cole (unpublished); J. Feinleib, W J. Scouler, and A. Ferretti, Phys. Rev. 165, 765 (1968).
[12] J. T. J. Huang and F. O. Ellison, Chem. Phys. 7, 473 (1975).
[13] M. J. S. Dewar, A. Komormicki, W. Thiel, and A. Schweig; Chem. Phys. Lett. 31, 286 (1975).
[14] A. Schweig and W. Thiel, J. Chem. Phys. 60, 951 (1974).
[15] F. R. Mc Feely, J. Stöhr, G. Apai, P. S. Wehner, and D. A. Shirley, Phys. Rev. B 14, 3273 (1976).
[16] N. J. Shevchik, Phys. Rev. B 16, 3428 (1977).
[17] J. H. Scofield, J. Electron. Spectrosc. 8, 129 (1976).
[18] W. Braun, A. Goldmann, and M. Cardona, Phys. Rev. B 10, 5069 (1974).
[19] R. Prins, Chem. Phys. Lett. 19, 355 (1973).
[20] L. Ley, R. A. Pollak, F. R. McFeely, S. P. Kowalczyk, and D. A. Shirley, Phys. Rev. B 9, 600 (1974).